A High-Order Time Finite Element Method Applied to Structural Dynamics Problems

Thanh Xuan Nguyen[1(✉)] and Long Tuan Tran[2]

[1] National University of Civil Engineering, Hanoi, Vietnam
[2] College of Urban Works Construction, Hanoi, Vietnam

Abstract. The article proposes a high-order time finite element method based on the well-posed variation formulation that is equivalent to the conventional strong form of governing equations in structural dynamics. Three cases related to the term "high-order" include: the time finite element that is analogous to the spatial second-order beam element; the p-power of the time-to-go $(T-t)$ in the formulation of "stiffness" matrix and "nodal force" vector; and the combination of both of them. In each case, the element "stiffness" matrix and "nodal force" vector are established and shown in details with notes on practical implementations.

Keywords: High-order time finite element · Structural dynamics · Variation formulation

1 Introduction

Dynamic response of a structure to an external excitation is of great concern in practical analysis and design. When dealing with a dynamic problem, usually the finite element method or a modal superposition approach is used to spatially discretize the structure, hence to reduce the problem to a set of ordinary differential equations in time that can be solved with one of many time stepping approaches [1,2]. This kind of procedure is widely used in practice and fairly well understood. Generally, for solving a set of ordinary differential equations in time, there are mainly two classes of direct time integration methods: explicit and implicit. Implicit methods (such as ones in β-Newmark family, Houbolt's method, and Runge-Kutta method) possess unconditional stability, but may require much more computations than that needed for an explicit method. On the other hand, explicit methods are conditionally stable. When coupled with the conventional finite element (FE) computation, the step size in any explicit method depends on the FE spatial mesh size and thus requires more computational effort. For both implicit and explicit methods, *a priori* error analysis is often not easily available, since they are all derived in the spirit of finite difference. A review of implicit and explicit ones can be found in [3–5], just to name a few.

A different approach for dealing with dynamic problem, being less popular than the methods mentioned above, is to use of the time (or temporal) finite element method (TFEM). The time finite element (TFE) formulation has several potential advantages as it can be applicable to both energy equation, and directly to the equations of motion. It is the straightforward derivation of higher order approximations in time. A key advantage of time finite element method, and the one often overlooked in its past applications, is the ease in which the sensitivity of the transient response with respect to various design parameters can be obtained. Usually, the TFEM approximation yields an accuracy superior to that of more conventional time stepping schemes at same computational cost [6]. Furthermore, the formulation is easy and convenient for computer implementation. The pioneer approaches, based on Hamilton's Law of varying action, can date back to the research of Argyris and Scharpf, who employed Hermite cubic interpolation polynomials (akin to the beam finite element) to express the response over each time finite element [7]. The method, based on the Hamilton's principle, was applied to a single-degree-of-freedom system but no numerical examples were considered. Fried [8] applied this approach to study the transient response of a damped system and transient heat conduction in a slab. Fried used a step by step approach to avoid storing and working with large matrices. Zienkiewicz and Parekh [9] used a time finite element approach to solve heat conduction problems. The formulation was based on Galerkin procedure over a time interval. In [10], Hulbert also employed the time-discontinuous Galerkin method and incorporates stabilizing terms having least-squares form. A general convergence theorem can be proved in a norm stronger than the energy norm. French and Peterson [11] proposed a time-continuous finite element method by transforming the second-order differential equations into first-order ones. Some other researchers have presented the variational formulation by allowing the TFE solution to be discontinuous at the end of each time element interval. Tang and Sun [12] introduced a unified TFE framework for the numerical discretization of ordinary differential equations based on TFE methods. In [6], Park used a bi-linear formulation for developing the time finite element method to obtain transient responses of both linear, nonlinear, damped and undamped systems. The sensitivity of the response with respect to various design parameters was also established. Results for both the transient response and its sensitivity to system parameters, when compared to a previously available approach that employs a multi-step method, are excellent. Recently, Wang and Zhong [13] proposed a time continuous Galerkin finite element method for structural dynamics. Its convergence property was proved through an a priori error analysis.

To the best of our knowledge, the time finite elements already available until now are just of the first-order kind under the view of time discretization. Thus the authors will propose in this article some developments of high-order time finite elements based on the well-posed variational formulation. Three cases related to the term "high-order" include: the time finite element that is analogous to the spatial second-order beam element; the p-power of the time-to-go $(T - t)$ in the formulation of "stiffness" matrix and "nodal force" vector; and the combination of both of them. The rest of the article is as follows. In Sect. 2, variational

formulation for structural dynamics is presented, followed by the first-order time finite element in Sect. 3. In Sect. 4, we propose high-order time finite elements in the above mentioned three cases. A numerical example is shown in Sect. 5, to illustrate the use of proposed high-order time finite elements in solving an SDOF dynamic problem. The article finalize with conclusions in Sect. 6.

2 Variational Formulation for Structural Dynamics

Consider a structure having n degrees of freedom in the time interval $\mathsf{L}_T = \,]0, T[$. The mass matrix $\mathbf{M} \in \mathbb{R}^{n \times n}$, and stiffness matrix $\mathbf{K} \in \mathbb{R}^{n \times n}$ are, generally, symmetric and positive definite. The damping matrix $\mathbf{C} \in \mathbb{R}^{n \times n}$ is, generally, symmetric non-negative definite. The structure is subjected to initial conditions $\mathbf{u}_0$ and $\dot{\mathbf{u}}_0$, in addition to an external load $\mathbf{F} \in L^2\,(\mathsf{L}_T)$, where $L^2\,(\mathsf{L}_T)$ is denoted for the Hilbert space on the time interval L_T. The governing equations with the unknown $\mathbf{u}$ is

$$\mathscr{L}\mathbf{u} \equiv \mathbf{M}\ddot{\mathbf{u}} + \mathbf{C}\dot{\mathbf{u}} + \mathbf{K}\mathbf{u} = \mathbf{F}, \qquad \mathbf{u}\,(0) = \mathbf{u}_0, \ \dot{\mathbf{u}}\,(0) = \dot{\mathbf{u}}_0 \tag{1}$$

Denote $H^2\,(\mathsf{L}_T)$ as the Sobolev space of order two. We introduce the two spaces as follows

$$H^2_{0p}\,(\mathsf{L}_T) = \left\{ \mathbf{u} \in H^2\,(\mathsf{L}_T) : \mathbf{u}\,(0) = \mathbf{u}_0, \dot{\mathbf{u}}\,(0) = \dot{\mathbf{u}}_0 \right\} \tag{2}$$

$$H^2_{00}\,(\mathsf{L}_T) = \left\{ \mathbf{u} \in H^2\,(\mathsf{L}_T) : \mathbf{u}\,(0) = \mathbf{0}, \dot{\mathbf{u}}\,(0) = \mathbf{0} \right\} \tag{3}$$

Also, an energy norm $\|\mathbf{v}\|_E : H^2\,(\mathsf{L}_T) \mapsto \mathbb{R}$ of a vector $\mathbf{v}$ is defined as

$$\|\mathbf{v}\|^2_E = \int_0^T \left(\frac{1}{2}\dot{\mathbf{v}}^T \mathbf{M}\dot{\mathbf{v}} + \frac{1}{2}\mathbf{v}^T \mathbf{K}\mathbf{v} \right) \mathrm{d}t \tag{4}$$

The following two theorems were proved in [13].

Theorem 1 (Variational formulation for structural dynamics)**.** The strong form of structural dynamics in the above equation is equivalent to the following formulation: find $\mathbf{u} \in H^2_{0p}\,(\mathsf{L}_T)$ such that

$$B\,(\mathbf{u}, \mathbf{v}) = \ell\,(\mathbf{v}), \qquad \forall \mathbf{v} \in H^2_{00}\,(\mathsf{L}_T) \tag{5}$$

where

$$B\,(\mathbf{u}, \mathbf{v}) = \int_0^T \int_0^s \dot{\mathbf{v}}^T \left(\mathbf{M}\ddot{\mathbf{u}} + \mathbf{C}\dot{\mathbf{u}} + \mathbf{K}\mathbf{u}\right) \mathrm{d}t\,\mathrm{d}s = \int_0^T (T - t)\,\dot{\mathbf{v}}^T \left(\mathbf{M}\ddot{\mathbf{u}} + \mathbf{C}\dot{\mathbf{u}} + \mathbf{K}\mathbf{u}\right) \mathrm{d}t \tag{6}$$

$$\ell\,(\mathbf{v}) = \int_0^T \int_0^s \dot{\mathbf{v}}^T \mathbf{F}\,\mathrm{d}t\,\mathrm{d}s = \int_0^T (T - t)\,\dot{\mathbf{v}}^T \mathbf{F}\,\mathrm{d}t \tag{7}$$

Theorem 2 (Solution estimation)**.** The following estimate for solution from the variational formulation

$$\|\mathbf{u}\|_E \le C\,(\|\mathbf{F}\|_0 + |\mathbf{u}_0| + |\dot{\mathbf{u}}_0|) \tag{8}$$

holds, where C denotes a positive constant (independent of mesh size or time step size), $\|\cdot\|_0$ is the usual norm of $L^2\,(\mathsf{L}_T)$ and $|\cdot|$ is defined as the usual length of a vector.

3 First-Order Time Finite Element

Let the interval $[0, T]$ be divided into a finite number N of non-overlap subintervals each of which has the length of T_i. Denote $H^2_{0p,\tau}(L_T)$ and $H^2_{00,\tau}(L_T)$ as the finite dimensional sub-spaces of $H^2_{0p}(L_T)$ and $H^2_{00}(L_T)$, respectively. Usually, $H^2_{0p,\tau}(L_T)$ and $H^2_{00,\tau}(L_T)$ are assumed to be of polynomial forms in each element with degree $p \geq 2$. Then, the time (Galerkin) finite element formulation is established by referring to the variational formulation (5): find $\mathbf{u}_\tau \in H^2_{0p,\tau}(L_T)$ such that

$$B(\mathbf{u}_\tau, \mathbf{v}_\tau) = \ell(\mathbf{v}_\tau), \qquad \forall \mathbf{v}_\tau \in H^2_{00,\tau}(L_T) \tag{9}$$

Well-posedness of the time FEM (9) is directly implicated in Theorem 1 and 2.

Generally, in structural dynamics, we consider both displacement and velocity responses, and moreover, $\mathbf{u}_\tau \in H^2(L_T)$. Thus, the Hermitian interpolation functions are suitable for establishing the time finite element. In [13], the first-order time finite element was obtained using Hermitian interpolation of degree $p = 3$, that is, for the ith element

$$\mathbf{u}_\tau = H_1 \mathbf{u}_b + H_2 \frac{T_i}{2} \dot{\mathbf{u}}_b + H_3 \mathbf{u}_e + H_4 \frac{T_i}{2} \dot{\mathbf{u}}_e = \mathbf{Hq}, \qquad \tau \in [0, T_i] \tag{10}$$

where $\mathbf{u}_b, \dot{\mathbf{u}}_b$ and $\mathbf{u}_e, \dot{\mathbf{u}}_e$ are, respectively, nodal (displacement and velocity) responses at the beginning and at the end of the time interval $[0, T_i]$ of that element. Vector $\mathbf{q}$ collects all the nodal responses in element i. The Hermitian interpolation functions - the shape functions - are as usual given as follows

$$H_1(\xi) = \frac{1}{4}(1-\xi)^2(2+\xi) \qquad H_2(\xi) = \frac{1}{4}(1+\xi)(1-\xi)^2 \tag{11}$$

$$H_3(\xi) = \frac{1}{4}(1+\xi)^2(2-\xi) \qquad H_4(\xi) = -\frac{1}{4}(1+\xi)^2(1-\xi) \tag{12}$$

where $\xi = (-1 + 2\tau/T_i) \in [-1, 1]$. Then, element stiffness matrix $\mathfrak{K}$ and nodal element load vector $\mathfrak{f}$ are obtained as follows

$$\mathfrak{K} = \int_0^{T_i} (T-t) \dot{\mathbf{H}}^T \left(\mathbf{M}\ddot{\mathbf{H}} + \mathbf{C}\dot{\mathbf{H}} + \mathbf{KH} \right) dt \tag{13}$$

$$\mathfrak{f} = \int_0^{T_i} (T-t) \dot{\mathbf{H}}^T \mathbf{F} \, dt \tag{14}$$

Now, by usual assembly process as seen in conventional finite element method, a set of algebraic equations is established. Also, the initial displacement and velocity are taken into account and entered to the formulation as the *boundary* conditions of the problem. After these steps, the *nodal* displacement and velocity at each instant of time can be obtained by solving

$$\mathfrak{K}^{\text{sys}} \mathbf{q}^{\text{sys}} = \mathfrak{f}^{\text{sys}} \tag{15}$$

It is noteworthy that the global *stiffness* matrix $\mathfrak{K}^{\text{sys}}$ is a block diagonal matrix and therefore, Eq. (15) can be efficiently solved by several usual algorithms, including the parallel method [13].
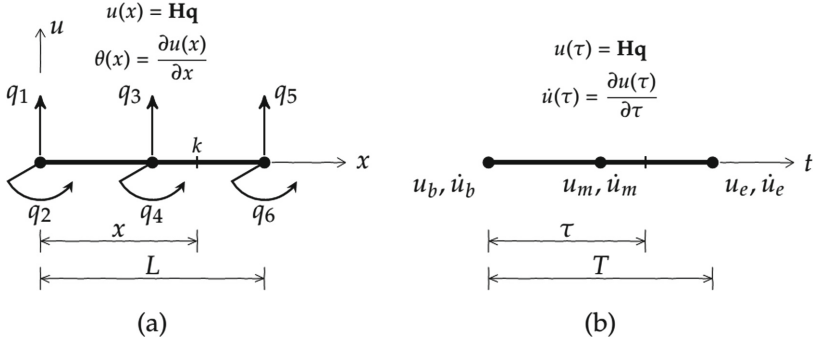
4   High-Order Time Finite Elements

In this section, we propose three high-order time finite elements. The first one, denoted as *2-order b-TFE*, is a direct extension of the first-order time finite element above, and adapted analogously to the second-order beam element with three equidistant nodes (see Fig. 1). Normally, the finite elements of order larger than two are not commonly used in practice since they might destroy the simple philosophy of the finite element method. In stimulating the concept of second-order beam element in conventional method, the following Hermitian interpolation functions are chosen as

$$H_1(\xi) = 1 - 23\xi^2 + 66\xi^3 - 68\xi^4 + 24\xi^5 \quad H_2(\xi) = \left(\xi - 6\xi^2 + 13\xi^3 - 12\xi^4 + 4\xi^5\right) T_i \quad (16)$$

$$H_3(\xi) = 16\xi^2 - 32\xi^3 + 16\xi^4 \qquad\qquad H_4(\xi) = \left(-8\xi^2 + 32\xi^3 - 40\xi^4 + 16\xi^5\right) T_i \quad (17)$$

$$H_5(\xi) = 7\xi^2 - 34\xi^3 + 52\xi^4 - 24\xi^5 \qquad H_6(\xi) = \left(-\xi^2 + 5\xi^3 - 8\xi^4 + 4\xi^5\right) T_i \quad (18)$$

where $\xi = \tau/T_i \in [0,1]$, and T_i is the "length" of the ith element. The three nodes in this element might not be equidistantly located. However, under practical view, the use of elements having non-equidistantly located nodes are not common. Also, we could otherwise use hierarchical functions as interpolation ones. However, if the isoparametric element is intended, then the ξ-t relationship is complex enough so that the advantage of using hierarchical polynomials in saving computational efforts might be lost.

With the element nodal responses $\mathbf{q}^T = \begin{bmatrix} \mathbf{u}_b^T \ \dot{\mathbf{u}}_b^T \ \mathbf{u}_m^T \ \dot{\mathbf{u}}_m^T \ \mathbf{u}_e^T \ \dot{\mathbf{u}}_e^T \end{bmatrix}$, the response $\mathbf{u}_\tau$ for the ith element can be interpolated from the above Hermitian functions. The formula for the matrix $\mathbf{H}$ in Eq. (10) varies case by case, since it depends on the number of degrees of freedom. For example, if the system is single-degree-of-freedom, then matrix $\mathbf{H}$ in Eq. (10) is defined as

$$\mathbf{H} = \begin{bmatrix} H_1 \ H_2 \ H_3 \ H_4 \ H_5 \ H_6 \end{bmatrix} \quad (19)$$

meanwhile if the system has n degree-of-freedom, then

$$\mathbf{H} = \begin{bmatrix} H_1 & & & H_2 & & & & H_6 & \\ & H_1 & & & H_2 & & & & H_6 \\ & & \ddots & & & \ddots & \cdots & & & \ddots \\ & & H_1 & & & H_2 & & & & H_6 \end{bmatrix} \quad (20)$$

$$\underbrace{\hphantom{H_1}}_{\text{diag. matrix of size } n} \underbrace{\hphantom{H_2}}_{\text{diag. matrix of size } n} \underbrace{\hphantom{H_6}}_{\text{diag. matrix of size } n}$$

Now, we follow Eqs. (13) and (14) for all time elements in the temporal mesh. In these equations, the time derivatives of $\mathbf{H}$ are given as

$$\dot{\mathbf{H}} = \frac{1}{T_i} \frac{d\mathbf{H}}{d\xi}, \qquad \ddot{\mathbf{H}} = \frac{1}{T_i^2} \frac{d^2\mathbf{H}}{d\xi^2} \quad (21)$$

The explicit formulae for the resulting element "stiffness" matrix and element "equivalent force" vector also vary case by case, since they are functions of the

Fig. 1. (a) Conventional (spatial) three-node beam finite element; and (b) Corresponding three-node time finite element

$\mathbf{M}$, $\mathbf{C}$, and $\mathbf{K}$ matrices obtained from spatial discretization as well. We observe here that a large intermediate manipulations of matrices for the element matrices (stiffness matrix and equivalent force vector) should be conducted. However, in practical implementation, we can take the advantage of sparsity in matrix $\mathbf{H}$ in these computations. In addition, these computations are prepared just once. For an n-DOF system, the resulting element time "stiffness" matrix is $6n \times 6n$, and that of "equivalent force" vector is $6n \times 1$.

When all element matrices are already determined, the global stiffness matrix and global equivalent force vector can be found by usual assembling procedure as in conventional finite element method.

The second time finite element, denoted as p-*TFE*, is based on the following observations. As we can see from Theorem 1, Eq. (5) is simply posed to be the residual $\mathscr{L}\mathbf{u} - \mathbf{F}$ weighted by a time dependent function $(T - t)\dot{\mathbf{v}}$, which is a product of the time-to-go $(T - t)$ and the test on-going velocity $\dot{\mathbf{v}}$. It raises to the idea that another time dependent function can be used as the weight. This idea is also supported by the fact (see proof at the Appendix)

$$\int_0^T \underbrace{\int_0^{s_1} \cdots \int_0^{s_p}}_{p\,\text{folds}} f \mathrm{d}t \, \mathrm{d}s_p \ldots \mathrm{d}s_1 = \int_0^T (T - t)^p f(t) \, \mathrm{d}t \qquad (22)$$

Thus, Eq. (5) in Theorem 1 holds with the bi-linear form $B : H^2(\mathrm{L}_T) \times H^2(\mathrm{L}_T) \mapsto \mathbb{R}$ and linear functional $\ell : H^2(\mathrm{L}_T) \mapsto \mathbb{R}$ expressed as below

$$B(\mathbf{u}, \mathbf{v}) = \int_0^T \underbrace{\int_0^{s_1} \cdots \int_0^{s_p}}_{p\,\text{folds}} \dot{\mathbf{v}}^T (\mathbf{M}\ddot{\mathbf{u}} + \mathbf{C}\dot{\mathbf{u}} + \mathbf{K}\mathbf{u}) \, \mathrm{d}t \, \mathrm{d}s_p \ldots \mathrm{d}s_1 \qquad (23)$$

$$= \int_0^T (T - t)^p \dot{\mathbf{v}}^T (\mathbf{M}\ddot{\mathbf{u}} + \mathbf{C}\dot{\mathbf{u}} + \mathbf{K}\mathbf{u}) \, \mathrm{d}t \qquad (24)$$

$$\ell\left(\mathbf{v}\right) = \int_0^T \underbrace{\int_0^{s_1} \cdots \int_0^{s_p}}_{p\,\text{folds}} \dot{\mathbf{v}}^T \mathbf{f}\, \mathrm{d}t\, \mathrm{d}s = \int_0^T (T-t)^p\, \dot{\mathbf{v}}^T \mathbf{f}\, \mathrm{d}t \qquad (25)$$

Supported by this, as before, we have the element "stiffness" matrix and the element "equivalent force" vector where the time-to-go $(T-t)$ is raised to the power of p as follows

$$\boldsymbol{\mathfrak{K}} = \int_0^{T_i} (T-t)^p\, \dot{\mathbf{H}}^T \left(\mathbf{M}\ddot{\mathbf{H}} + \mathbf{C}\dot{\mathbf{H}} + \mathbf{K}\mathbf{H}\right) \mathrm{d}t \qquad (26)$$

$$\mathfrak{f} = \int_0^{T_i} (T-t)^p\, \dot{\mathbf{H}}^T \mathbf{F}\, \mathrm{d}t \qquad (27)$$

We see that, in this formulation, the specific types of "shape" functions will give different variants of the element matrices. For the second type of time finite element proposed in this article, the common Hermitian interpolation polynomials of degree 3 are used. For SDOF system $n = 1$, the element "stiffness" matrix is shown in the Appendices section. When the six "shape" functions in Eqs. (16)–(18) are used, then we have the third type of time finite element, which is a combination of the second-order beam analogous element and the "p-power of the time-to-go" element. This type of element is denoted as *bp-TFE* for later reference. It is too lengthy to show the formulas of element "stiffness" matrix and "equivalent force" vector here. Instead, MATLAB code to obtain these quantities are given in the Appendices section.

5   Numerical Example

In this section, we will illustrate the use of proposed high-order TFEs in solving an undamped single-degree-of-freedom (SDOF) dynamic problem. Out of the accuracy aspect, we will not explore all other aspects of numerical performance of the proposed method through this very example. For comparison, the problem is also solved by Newmark-β method - the most popular numerical integration method for transient structural dynamics - with three different sets of parameters (γ, β), namely $(1/2, 0)$, $(1/2, 1/6)$, and $(1/2, 1/4)$. The most accurate results obtained by using Newmark-β methods with these sets of parameters are shown in Table 1 and Table 2. The results offered by [13] are also taken into the comparison of accuracy.

The statement of the problem is as follows. Given a SDOF system having the mass of $m = 1$, the stiffness of $k = \pi^2/4$, and there is no damping $c = 0$. The system is at rest when it is suddenly enforced by a pulse force $f(t)$ given below

$$f\left(t\right) = \begin{cases} 1, & 0 < t < 1 \\ 0, & t \geq 1 \end{cases}$$

The exact displacement and velocity responses of the system are found to be

$$u\left(t\right) = \begin{cases} 4\left(1 - \cos\pi t/2\right)/\pi^2, & 0 < t < 1 \\ 4\left(\sin\pi t/2 - \cos\pi t/2\right)/\pi^2, & t \geq 1 \end{cases}$$

and

$$\dot{u}\left(t\right) = \begin{cases} 2\left(\sin\pi t/2\right)/\pi, & 0 < t < 1 \\ 2\left(\cos\pi t/2 + \sin\pi t/2\right)/\pi, & t \geq 1 \end{cases}$$

The responses over the time interval $[0, T]$ are considered, where $T = 12$ s. The time interval $[0, T]$ is uniformly divided into N elements such that mesh size is $\tau = T/N$. Five different mesh sizes are considered, namely $\tau = 1; 1/2; 1/4; 1/8;$ and $1/16$. For each mesh size, to quantify specifically the accuracy, discrete max-norm errors, defined as maximum of absolute point-wise errors at all time nodes are computed and listed in Table 1 for displacement responses and in Table 2 for velocity responses.

Table 1. Discrete max-norm error in displacement with the use of Newmark (γ, β) method; first-order TFEs, high-order p-TFEs, and high-order bp-TFEs

Mesh size τ		1	1/2	1/4	1/8	1/16
Newmark (γ, β)		$6.8035 \cdot 10^{-1}$	$2.0725 \cdot 10^{-1}$	$5.6488 \cdot 10^{-2}$	$1.4457 \cdot 10^{-2}$	$3.6345 \cdot 10^{-3}$
1st-order TFEs [13]		$5.5966 \cdot 10^{-3}$	$5.6461 \cdot 10^{-4}$	$6.0392 \cdot 10^{-5}$	$1.0574 \cdot 10^{-5}$	$2.3831 \cdot 10^{-6}$
p-TFEs	$p = 0$	$1.7453 \cdot 10^{-2}$	$4.2177 \cdot 10^{-3}$	$1.0449 \cdot 10^{-3}$	$2.6062 \cdot 10^{-4}$	$6.5117 \cdot 10^{-5}$
	$p = 2$	$6.3392 \cdot 10^{-3}$	$4.8783 \cdot 10^{-4}$	$5.3554 \cdot 10^{-5}$	$1.0934 \cdot 10^{-5}$	$2.6293 \cdot 10^{-6}$
	$p = 3$	$7.4930 \cdot 10^{-3}$	$5.6636 \cdot 10^{-4}$	$5.2995 \cdot 10^{-5}$	$4.3692 \cdot 10^{-6}$	$3.3646 \cdot 10^{-7}$
bp-TFEs	$p = -1$	$1.3646 \cdot 10^{-4}$	$7.5843 \cdot 10^{-6}$	$4.8081 \cdot 10^{-7}$	$2.9627 \cdot 10^{-8}$	$1.8455 \cdot 10^{-9}$
	$p = 0$	$1.7552 \cdot 10^{-4}$	$1.0379 \cdot 10^{-5}$	$6.4020 \cdot 10^{-7}$	$3.9883 \cdot 10^{-8}$	$2.4914 \cdot 10^{-9}$
	$p = 1$	$6.3564 \cdot 10^{-4}$	$3.7165 \cdot 10^{-5}$	$2.2662 \cdot 10^{-6}$	$1.4023 \cdot 10^{-7}$	$8.7608 \cdot 10^{-9}$
	$p = 2$	$1.7412 \cdot 10^{-3}$	$9.9408 \cdot 10^{-5}$	$5.9858 \cdot 10^{-6}$	$3.6814 \cdot 10^{-7}$	$2.2857 \cdot 10^{-8}$
	$p = 3$	$4.6406 \cdot 10^{-3}$	$2.6035 \cdot 10^{-4}$	$1.6075 \cdot 10^{-5}$	$9.8146 \cdot 10^{-7}$	$6.0857 \cdot 10^{-8}$

Table 2. Discrete max-norm error in velocity with the use of Newmark (γ, β) method; first-order TFEs, high-order p-TFEs, and high-order bp-TFEs

Mesh size τ		1	1/2	1/4	1/8	1/16
Newmark (γ, β)		$1.0997 \cdot 10^{0}$	$3.4703 \cdot 10^{-1}$	$9.7632 \cdot 10^{-2}$	$2.5006 \cdot 10^{-2}$	$6.2638 \cdot 10^{-3}$
1st-order TFEs [13]		$4.3783 \cdot 10^{-2}$	$1.0041 \cdot 10^{-2}$	$2.4368 \cdot 10^{-3}$	$6.0898 \cdot 10^{-4}$	$1.5183 \cdot 10^{-4}$
p-TFEs	$p = 0$	$8.5147 \cdot 10^{-2}$	$2.0884 \cdot 10^{-2}$	$5.3131 \cdot 10^{-3}$	$1.3232 \cdot 10^{-3}$	$3.3096 \cdot 10^{-4}$
	$p = 2$	$6.1716 \cdot 10^{-2}$	$1.0608 \cdot 10^{-2}$	$2.6661 \cdot 10^{-3}$	$6.5878 \cdot 10^{-4}$	$1.6481 \cdot 10^{-4}$
	$p = 3$	$1.0299 \cdot 10^{-1}$	$1.3080 \cdot 10^{-2}$	$2.5550 \cdot 10^{-3}$	$6.3140 \cdot 10^{-4}$	$1.5739 \cdot 10^{-4}$
bp-TFEs	$p = -1$	$4.5059 \cdot 10^{-4}$	$3.1248 \cdot 10^{-5}$	$1,9402 \cdot 10^{-6}$	$1.2238 \cdot 10^{-7}$	$7.6559 \cdot 10^{-9}$
	$p = 0$	$8.2538 \cdot 10^{-4}$	$5.0875 \cdot 10^{-5}$	$3.2486 \cdot 10^{-6}$	$2.0238 \cdot 10^{-7}$	$1.2658 \cdot 10^{-8}$
	$p = 1$	$1.7616 \cdot 10^{-3}$	$1.0278 \cdot 10^{-4}$	$6.2780 \cdot 10^{-6}$	$3.9268 \cdot 10^{-7}$	$2.4459 \cdot 10^{-8}$
	$p = 2$	$4.1561 \cdot 10^{-2}$	$2.3697 \cdot 10^{-4}$	$1.4289 \cdot 10^{-5}$	$8.8230 \cdot 10^{-7}$	$5.4853 \cdot 10^{-8}$
	$p = 3$	$1.0311 \cdot 10^{-2}$	$5.7400 \cdot 10^{-4}$	$3.5423 \cdot 10^{-5}$	$2.1650 \cdot 10^{-6}$	$1.3393 \cdot 10^{-7}$

The b-TFEs are the special case of bp-TFEs when $p = 1$. Comparing the results offered by [13] with ones obtained by using b-TFEs, we can see that for all mesh sizes considered, the b-TFEs give much more accurate results. The smaller the mesh size is, the higher magnitude order of accuracy can be observed. There is also an interesting observation. Although the cases when $p = -1$ or $p = 0$ are not supported by strictly mathematical arguments, the numerical results obtained in these two cases with bp-TFEs are still more accurate than that obtained with bp-TFEs when $p \in N, p \geq 1$.

For the p-TFEs, the results are somewhat disappointing and unpredictable. Although there are some cases that p-TFEs can defeat the first-order TFEs (for example, when $p = 3$ and the mesh size $\tau = 1/8$ or $1/16$), the overall performance of p-TFEs is worse, compared with the first-order TFEs, in many other cases with different values of p and τ. Moreover, different from the case of using bp-TFEs, the trial of using p-TFEs with $p = -1$ failed, since the obtained matrix is close to singular.

6   Conclusions

The equation obtained from the well-posed variational statement for structural dynamics can be regarded as the governing equation in weighted residual methods, where the weight function is a time-dependent one. Based on this observation, several high-order time finite elements have been proposed in this work, namely the 2-order b-TFE, the p-TFE, and the combined 2-order pb-TFE. The expressions for the element "stiffness" matrix and "equivalent force" vector were shown in details with notes on practical implementation. The performance of high-order TFEs, such as stability, accuracy and convergence, compared to previous methods are being under investigation and will be presented in the next article. It is believed that TFEM with these high-order type of element would be effective tool for structural dynamic analysis.

APPENDICES

1   The Proof of Equations (24) and (25)

$$\int_0^T \underbrace{\int_0^{s_1} \cdots \int_0^{s_p}}_{p\,\text{folds}} f\,\mathrm{d}t\,\mathrm{d}s_p \ldots \mathrm{d}s_1 = -\int_0^T \frac{\mathrm{d}\,(T - s_1)}{\mathrm{d}s_1} \left(\underbrace{\int_0^{s_1} \cdots \int_0^{s_p}}_{p\,\text{folds}} f\,\mathrm{d}t\,\mathrm{d}s_p \ldots \mathrm{d}s_2 \right) \mathrm{d}s_1$$

$$= -\left\{ (T - s_1) \underbrace{\int_0^{s_1} \cdots \int_0^{s_p}}_{p\,\text{folds}} f\,\mathrm{d}t\,\mathrm{d}s_p \ldots \mathrm{d}s_2 \right\} \Bigg|_{s_1=0}^{T} + \int_0^T (T - s_1) \frac{\mathrm{d}\left(\underbrace{\int_0^{s_1} \cdots \int_0^{s_p}}_{p\,\text{folds}} f\,\mathrm{d}t\,\mathrm{d}s_p \ldots \mathrm{d}s_2 \right)}{\mathrm{d}s_1} \mathrm{d}s_1$$

$$= \int_0^T (T - s_1) \frac{d \left(\underbrace{\int_0^{s_1} \cdots \int_0^{s_p} f dt\, ds_p \ldots ds_2}_{p\ \text{folds}} \right)}{ds_1} ds_1 = \int_0^T (T - s_1) \underbrace{\int_0^{s_2} \cdots \int_0^{s_p} f ds_p \ldots ds_2 ds_1}_{(p-1)\ \text{folds}}$$

$$= \int_0^T \underbrace{\int_0^{s_2} \cdots \int_0^{s_p}}_{(p-1)\ \text{folds}} (T - t)\, f dt\, ds_p \ldots ds_2 = \cdots = \int_0^T (T - t)^p\, f(t)\, dt$$

The rest of the proof is straightforward.

2 Element "Stiffness" Matrix of p-TFE for SDOF System

We observe that the "equivalent force" vector also has the term T^p, thus in practical implementation, we can cancel this term out from both sides. The following results are obtained from symbolic computation in MATLAB, with the common term T^{p-2} in both sides of Eq. (15) canceled out.

$$f_1(p) = 1/\left(p^3 + 9p^2 + 26p + 24\right)$$
$$f_2(p) = 1/\left(p^3 + 12p^2 + 47p + 60\right)$$
$$f_3(p) = 1/\left(p^3 + 15p^2 + 74p + 120\right)$$
$$f_4(p) = 1/\left(p^4 + 10p^3 + 35p^2 + 50p + 24\right)$$
$$f_5(p) = 1/\left(p^4 + 14p^3 + 71p^2 + 154p + 120\right)$$
$$f_6(p) = 1/\left(p^4 + 18p^3 + 119p^2 + 342p + 360\right)$$
$$f_7(p) = 1/\left(p^5 + 15p^4 + 85p^3 + 225p^2 + 274p + 120\right)$$
$$f_8(p) = 1/\left(p^5 + 18p^4 + 121p^3 + 372p^2 + 508p + 240\right)$$
$$f_9(p) = 1/\left(p^5 + 20p^4 + 155p^3 + 580p^2 + 1044p + 720\right)$$

$$\mathbf{h}_m = 2 \begin{bmatrix} 18pf_1 & 12(p+1)Tf_1 & -18pf_1 & 6(p-2)Tf_1 \\ -3(p^2+2p+4)Tf_1 & -(2p^2+5p+6)T^2f_1 & 3(p^2+2p+4)Tf_1 & -(p^2+p+6)T^2f_1 \\ -18pf_1 & -12(p+1)Tf_1 & 18pf_1 & -6(p-2)Tf_1 \\ 6(p^2+2)Tf_4 & 2(2p^2+2p+3)T^2f_4 & -6(p^2+2)Tf_4 & 2(p^2-2p+3)T^2f_4 \end{bmatrix}$$

$$\mathbf{h}_c = T \begin{bmatrix} 72f_2 & -6(p-1)Tf_2 & -72f_2 & 12(2p+1)Tf_5 \\ -6(p-1)Tf_2 & (p^2+3p+8)T^2f_2 & 6(p-1)Tf_2 & -2(p^2+2)T^2f_5 \\ -72f_2 & 6(p-1)Tf_2 & 72f_2 & -12(2p+1)Tf_5 \\ 12(2p+1)Tf_5 & -2(p^2+2)T^2f_5 & -12(2p+1)Tf_5 & 8(p^2+2)T^2f_7 \end{bmatrix}$$

$$\mathbf{h}_k = T^2 \begin{bmatrix} -6(p+10)f_3 & -12Tf_3 & -36(3p+10)f_9 & 36Tf_6 \\ (p^2+10p+12)Tf_3 & pT^2f_3 & 6(p^2-12)Tf_9 & -2(p-3)T^2f_6 \\ 6(p+10)f_3 & 12Tf_3 & 36(3p+10)f_9 & -36Tf_6 \\ -2(p^2+12p+18)Tf_6 & -2(2p+3)T^2f_6 & -12(3p-2)Tf_8 & 12pT^2f_9 \end{bmatrix}$$

$$\mathbf{\mathcal{K}} = m\mathbf{h}_m + c\mathbf{h}_c + k\mathbf{h}_k$$

3 MATLAB Code for Obtaining "Stiffness" Matrix of bp-TFE for SDOF Systems

```
syms xi p T m c k tb Ti
assume (p > 0);
assume (Ti > 0);
H1(xi) = 24 * xi^5 - 68 * xi^4 + 66 * xi^3 - 23 * xi^2 + 1;
H2(xi) = (4 * xi^5 - 12 * xi^4 + 13 * xi^3 - 6 * xi^2 + xi) * Ti;
H3(xi) = 16 * xi^5 - 32 * xi^4 + 16 * xi^2;
H4(xi) = (16 * xi^5 - 40 * xi^4 + 32 * xi^3 - 8 * xi^2) * Ti;
H5(xi) = -24 * xi^5 + 52 * xi^4 - 34 * xi^3 + 7 * xi^2;
H6(xi) = (4 * xi^5 - 8 * xi^4 + 5 * xi^3 - xi^2) * Ti;
H(xi) = [H1(xi) H2(xi) H3(xi) H4(xi) H5(xi) H6(xi)];
Hd(xi) = diff(H(xi),xi);
Hdd(xi) = diff(H(xi),xi,2);
h_m = 1/Ti^2 * int((T-tb-xi * Ti)^p.*transpose(Hd(xi)) * Hdd(xi), xi,0,1);
h_c = 1/Ti * int((T-tb-xi * Ti)^p.*transpose(Hd(xi)) * Hd(xi), xi,0,1);
h_k = int((T-tb-xi * Ti)^p.*transpose(Hd(xi)) * H(xi), xi,0,1);
K = m * h_m + c * h_c + k * h_k
```

References

1. Zienkiewicz, O.C.: A new look at the Newmark, Houboult and other time stepping formulas. A weighted residual approach. Earthq. Eng. Struct. Dynam. **5**, 413–418 (1977)
2. Newmark, N.M.: A method of computation for structural dynamics. Trans. Am. Soc. Civil Eng. **127**, 1406–1435 (1962)
3. Dokainish, M.A., Subbaraj, K.: A survey of direct time-integration methods in computational structural dynamics–I. Explicit methods. Comput. Struct. **32**, 1371–1386 (1989)
4. Subbaraj, K., Dokainish, M.A.: A survey of direct time-integration methods in computational structural dynamics–II. Implicit methods. Comput. Struct. **32**, 1387–1401 (1989)
5. Hughes, T.J.R., Belytschko, T.: A precis of developments in computational methods for transient analysis. ATJAM **50**, 1033–1041 (1983)
6. Park, S.: Development and applications of finite elements in time domain, Doctoral dissertation. Virginia Tech (1996)
7. Argyris, J.H., Scharpf, D.W.: Finite element in time and space. Aeronaut. J. Roy. Aeronaut. Soc. **73**, 1041–1044 (1969)
8. Fried, I.: Finite element analysis of time dependent phenomena. AIAA J. **7**, 1170–1173 (1969)
9. Zienkiewicz, O.C., Parekh, C.J.: Transient field problems-two and three dimensional analysis by isoparametric finite elements. Int. J. Numer. Methods Eng. **2**, 61–71 (1970)
10. Hulbert, G.M.: Time finite element methods for structural dynamics. Int. J. Numer. Methods Eng. **33**, 307–331 (1992)

11. French, D.A., Peterson, T.E.: A continuous space-time finite element method for the wave equation. Math. Comput. **65**, 491–506 (1996)
12. Tang, W., Sun, Y.: Time finite element methods: a unified framework for numerical discretizations of ODEs. Appl. Math. Comput. **219**, 2158–2179 (2012)
13. Wang, L., Zhong, H.: A time finite element method for structural dynamics. Appl. Math. Model. **41**, 445–461 (2017)